Chemical Engineering Science 59 (2004) 5795–5806

Chemical Engineering Science

www.elsevier.com/locate/ces

Identification of kinetic and thermodynamic reaction parameters from online calorimetric and IR-ATR data using a new combined evaluation algorithm

Andreas Zogg, Ulrich Fischer*, Konrad Hungerbühler

Saftey & Environmental Technology Group, Institute for Chemical and Bioengineering, Swiss Federal Institute of Technology (ETH), CH-8093 Zurich, Switzerland

Received 16 November 2003; received in revised form 17 June 2004; accepted 23 June 2004
Available online 3 September 2004

Abstract

In order to identify parameters of a chemical reaction, such as rate constants, reaction orders, activation energies, or reaction enthalpies, a new evaluation algorithm that allows a simultaneous evaluation of online measured infrared and calorimetric data will be investigated. The evaluation of the infrared data neither requires calibration nor the knowledge of pure component spectra. Overlapping absorption bands are allowed. The weighting of the calorimetric and infrared objective functions performs completely automatic using a sensitivity analysis. The performance of this combined evaluation principle was investigated by analyzing the consecutive epoxidation of 2,5-di-tert-butyl-1,4-benzoquinone with tert-butyl hydrogen peroxide. Different reaction models as well as physical constraints were postulated in order to reveal the flexibility and the capability of the approach. The results obtained underline the importance of such a combined evaluation of both analytical signals instead of separate evaluations.

Keywords: Reaction calorimetry; Infrared—ATR spectroscopy; Kinetic analysis; Parameter identification; Nonlinear optimization; Hard modeling; Thermodynamics; Multi-objective optimization; Epoxidation

1. Introduction

A standard analytical tool for the purpose of kinetic and thermodynamic reaction analysis is reaction calorimetry (Karlsen and Villadsen, 1987; Landau, 1996; Regenass, 1997; Zogg, 2003; Zogg et al., 2004b). As the heat release or uptake during a chemical reaction is proportional to the reaction rate, calorimetry can be compared to a differential kinetic analysis method (Levenspiel, 1998). To improve the information content of a single measurement, calorimetric devices are therefore often combined with an additional integral analytical sensor (proportional to the component concentrations) such as an IR-ATR-probe (Landau et al., 1995; LeBlond et al., 1998; am Ende et al., 1999; Ubrich et al., 1999; Nomen et al., 2001; Zogg et al., 2003; Ma et al., 2003). Both techniques do not require any sampling and are thus straightforward to apply. As the infrared spectra generally depend on the temperature, isothermal conditions are preferable. Otherwise, spectral shifts caused by temperature changes disturb the analysis and must be accounted for (Furusjö and Danielsson, 2000; Furusjö et al., 2003).

For the identification of the desired thermodynamic and kinetic reaction parameters of a specified empirical reaction model, mathematical evaluation methods are required. A detailed overview on these techniques is presented by Zogg (2003) focusing on the evaluation of isothermally measured reaction data. The evaluation of the calorimetric and infrared data is conventionally carried out separately (LeBlond

* Corresponding author. Tel.: +41-1-632-5668; fax: +41-1-632-1189.
E-mail address: ufischer@chem.ethz.ch (U. Fischer).

0009-2509/$ - see front matter © 2004 Elsevier Ltd. All rights reserved.
doi:10.1016/j.ces.2004.06.034

et al., 1998; Ubrich et al., 1999; Nomen et al., 2001; Zogg et al., 2003; Ma et al., 2003). However, the reaction parameters identified by separate evaluations of the calorimetric and infrared data can differ significantly (mostly the reasons are measurement errors, unequal information content, or unmodeled processes with different influence on the two analytical signals). Therefore, it is desirable to evaluate both data sets simultaneously in order to estimate all thermodynamic and kinetic reaction parameters in a single step, representing an overall optimal solution.

The crucial step in such a combined evaluation is to find an appropriate weighting of the two different analytical signals in order to equalize their influence on the estimated reaction parameters. A similar problem is encountered if calorimetric and concentration data are evaluated simultaneously (Machado et al., 1996; Fillion et al., 2002; BatchCAD,; ChemCad,; BatchReactor,). No systematic weighting procedure was reported to date. We developed an automatic and systematic scaling procedure that does not require any user interaction and is therefore attractive for practical applications. This new procedure was applied to isothermal measurements (17, 24, 30 and 36 °C) of the consecutive epoxidation of 2,5-di-tert-butyl-1,4-benzoquinone with tert-butyl-hydroperoxide. Three evaluations using different physical constraints, reaction models, and initial concentrations of the hydroperoxide were carried out. The evaluations do neither require any calibration of the infrared data nor any knowledge of the pure component spectra. The results show that it is essential to carry out a combined evaluation of both analytical signals using sensitivity analysis instead of separate evaluations.

2. Theory

In this study, the newly developed *Combined Evaluation Algorithm*, which will be explained below, was applied to the consecutive epoxidation of 2,5-di-tert-butyl-1,4-benzoquinone with tert-butyl-hydroperoxide. The scheme of this reaction is given in Fig. 1. This reaction was chosen as three independent kinetic studies are available (Hairfield et al., 1985; Mayes et al., 1992; Bijlsma et al., 1998). In order to allow a later comparison of the estimated rate constants to literature references, the concentrations of the educts were chosen similar to those of Mayes et al. (1992). In analogy to the studies of Hairfield et al. (1985); Mayes et al. (1992); Bijlsma et al. (1998), it was assumed that the concentration of tert-butyl hydroperoxide (in excess compared to the benzoquinone) remains constant during the reaction. The reaction model equations can thus be written as follows:

$$\frac{\mathrm{d}n_{\mathrm{Educt}}}{\mathrm{d}t} = -r_1(t,k_1)V_r(t) \qquad \frac{\mathrm{d}n_{\mathrm{Hydroperoxide}}}{\mathrm{d}t} = \{-r_1(t,k_1) - r_2(t,k_2)\}\,V_r(t)$$

$$\frac{\mathrm{d}n_{\mathrm{Mono\ Epoxide}}}{\mathrm{d}t} = \{r_1(t,k_1) - r_2(t,k_2)\}\,V_r(t)$$

$$\frac{\mathrm{d}n_{\mathrm{Di\ Epoxide}}}{\mathrm{d}t} = r_2(t,k_2)\,V_r(t)$$

$$\frac{\mathrm{d}n_{\mathrm{tButanol}}}{\mathrm{d}t} = \{r_1(t,k_1) + r_2(t,k_2)\}\,V_r(t)$$

$$\frac{\mathrm{d}n_{\mathrm{Solvent}}}{\mathrm{d}t} = 0 \qquad \frac{\mathrm{d}n_{\mathrm{Methanol}}}{\mathrm{d}t} = v_{\mathrm{dos}}\,c_{\mathrm{dos,\ Methanol}}$$

$$\frac{\mathrm{d}n_{\mathrm{Triton\ B}}}{\mathrm{d}t} = v_{\mathrm{dos}}\,c_{\mathrm{dos,\ Triton\ B}}$$

$$\frac{\mathrm{d}V_r}{\mathrm{d}t} = v_{\mathrm{dos}}$$

$$r_1(t,k_1) = k_1\,\frac{n_{\mathrm{Educt}}(t)}{V_r(t)}\,\frac{n_{\mathrm{Triton\ B}}(t)}{V_r(t)}\,c_{\mathrm{Hydroperoxide},0}$$

$$r_2(t,k_2) = k_2\,\frac{n_{\mathrm{Mono\ Epoxide}}(t)}{V_r(t)}\,\frac{n_{\mathrm{Triton\ B}}(t)}{V_r(t)}\,c_{\mathrm{Hydroperoxide},0} \qquad (1)$$

where n_j is the number of moles of component j (mol), V_r is the volume of the reaction mixture (l), r_i is the ith reaction rate (mol/l/s), k_i the ith rate constant ($\mathrm{l}^2/\mathrm{mol}^2/\mathrm{s}$), v_{dos} is the dosing rate (s^{-1}), $c_{\mathrm{dos,\ Methanol}}$ is the concentration of methanol in the feed, $c_{\mathrm{dos,\ Triton\ B}}$ is the concentration of the catalyst (Triton B). The concentration of the catalyst is included in r_1 and r_2, however, it varies only during the short addition phase (24 s) and remains constant during the rest of the experiment. In order to allow comparison to other literature data, the initial concentration of the hydroperoxide $c_{\mathrm{Hydroperoxide},0}$ is excluded from the rate constants (see below). As several isothermal experiments at different temperatures are evaluated at the same time, the rate constants k_1 and $k_2(=k_i)(\mathrm{l}^2/\mathrm{mol}^2/\mathrm{s})$ are calculated based on the following Arrhenius approximation:

$$k_i(T_r) = k_i(T_{\mathrm{ref}})\,\exp\left\{-\frac{E_{A,i}}{R}\left(\frac{1}{T_r} - \frac{1}{T_{\mathrm{ref}}}\right)\right\} \qquad (2)$$

where $E_{A,i}$ are the activation energies (J/mol), R is the ideal gas constant (J/mol/K), T_{ref} is the reference temperature (K), and T_r is the reaction temperature (K). Instead of the rate constants k_1 and k_2, two activation energies $E_{A,1}$ and $E_{A,2}$ as well as the two rate constants $k_1(T_{\mathrm{ref}})$ and $k_2(T_{\mathrm{ref}})$ at the reference temperature have to be identified. Furthermore, two reaction enthalpies $\Delta_r H_1$ and $\Delta_r H_2$ (J/mol) as well as the pure component spectra (different spectra for each temperature) of the eight components are assumed to be unknown.

The Combined Evaluation Algorithm (Fig. 2) is divided into an outer nonlinear least-squares optimization to identify the reaction model parameters (k_1, k_2, $E_{A,1}$, $E_{A,2}$ = kinetic reaction parameters; see Eq. (3)) and two inner linear least-squares optimizations: (i) the identification of the reaction

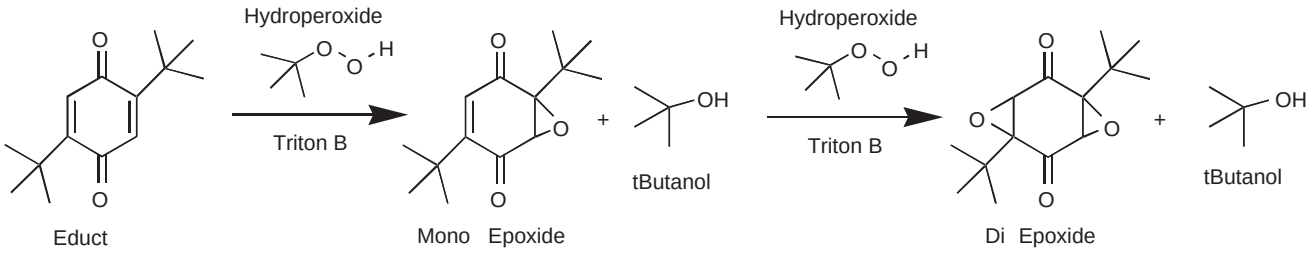

Fig. 1. Consecutive epoxidation of 2,5-di-tert-butyl-1,4-benzoquinone with tert-butyl-hydroperoxide. The catalyst was dosed to the reaction mixture to initiate the reaction.

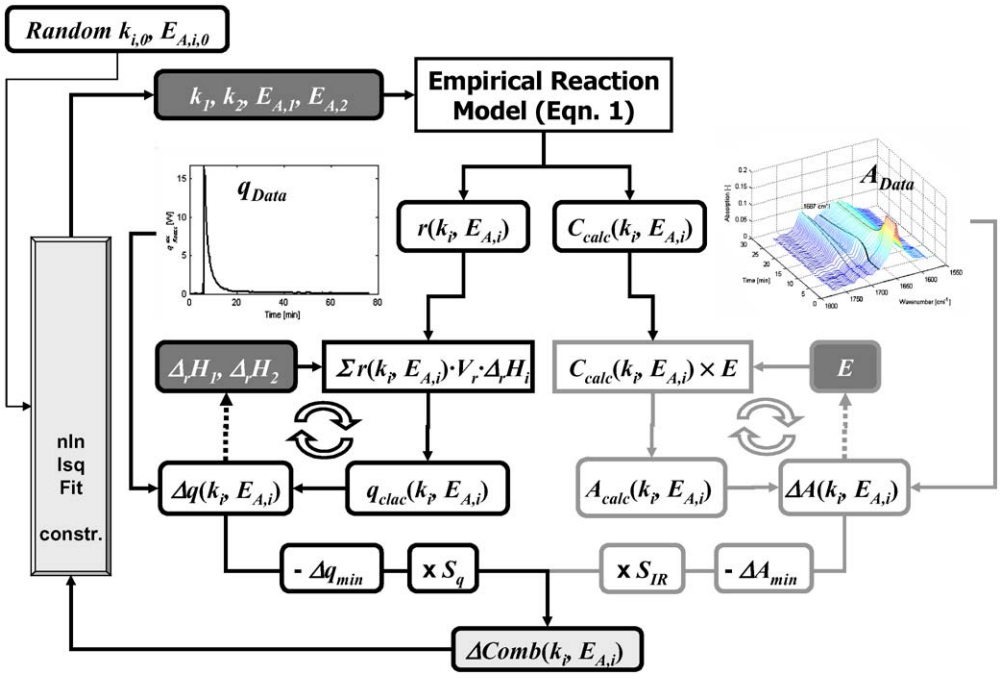

Fig. 2. Schematic representation of the Combined Evaluation Algorithm for the epoxidation reaction. The unknown rate constants k_i (k_1, k_2), activation energies $E_{A,i}$ $(E_{A,1},\ E_{A,2})$, reaction enthalpies $\Delta_r H_i$ $(\Delta_r H_1, \Delta_r H_2)$ as well as the unknown matrix of pure component spectra E are highlighted.

enthalpies ($\Delta_r H_1$, $\Delta_r H_2$ = thermodynamic reaction parameters; see Eq. (4)) and (ii) the identification of the pure spectra matrix E (spectroscopic reaction parameters; see Eqs. (6)–(9)):

$$\min_{k_1,k_2,E_{A,1},E_{A,2}} \{S_{IR}(\Delta A(k_1, k_2, E_{A,1}, E_{A,2}) - \Delta A_{\min}) + S_q(\Delta q(k_1, k_2, E_{A,1}, E_{A,2}) - \Delta q_{\min})\}, \quad (3)$$

where S_{IR} (dimensionless) and S_q $[W^{-2}]$ are scaling factors (see below), $\Delta q_{\min}(W^2)$ and $\Delta A_{\min}$ (dimensionless) are the minimal calorimetric and infrared error as defined in Eqs. (12) and (13), respectively.

$$\Delta q(k_1, k_2, E_{A,1}, E_{A,2}) = \min_{\Delta_r H_1, \Delta_r H_2} \left\{ \sum_{t=1}^{N_{t,q}} [q_{\text{Data},t} - q_{\text{Calc},t}]^2 \right\} \quad (4)$$

$$q_{\text{Calc}} = \sum_{i=1}^{2} V_r(-\Delta_r H_i)\, r_i(k_i, E_{A,i}), \quad (5)$$

where q_{Data} and q_{Calc} are the measured and calculated calorimetric data (W) (vector of length $N_{t,q}$), respectively, $N_{t,q}$ is the number of calorimetric time samples. The reaction rates r_i are calculated according to Eq. (1) (however, in contrast to Eq. (1), V_r and r_i are now vectors of length $N_{t,q}$). The linear minimization to calculate the reaction enthalpies $\Delta_r H_{1,2}$ is carried out using a constrained linear least-squares algorithm.

$$\Delta A(k_1, k_2, E_{A,1}, E_{A,2}) = \sum_{n=1}^{N_{\tilde{\nu}}} \Delta A_n(k_1, k_2, E_{A,1}, E_{A,2}), \quad (6)$$

$$\Delta A_n(k_1, k_2, E_{A,1}, E_{A,2}) = \min_{E_n} \left\{ \sum_{t=1}^{N_{t,IR}} [A_{\mathrm{Data},t,n} - A_{\mathrm{Calc},t,n}(k_1, k_2, E_{A,1}, E_{A,2}, E_n)]^2 \right\} \tag{7}$$

$$A_{\mathrm{Calc}}(k_1, k_2, E_{A,1}, E_{A,2}, E) = C_{\mathrm{Calc}}(k_1, k_2, E_{A,1}, E_{A,2}) \times E \tag{8}$$

$$C_{\mathrm{Calc}}(k_1, k_2, E_{A,1}, E_{A,2}) = [c_{\mathrm{Educt}}, \ldots, c_{\mathrm{Triton\ B}}] \quad E = \begin{bmatrix} e_{\mathrm{Educt}} \\ \vdots \\ e_{\mathrm{Triton\ B}} \end{bmatrix} \tag{9}$$

where A_{Data} and A_{Calc} are the measured and calculated infrared spectra (dimensionless) (matrix of dimension $N_{t,IR} \times N_{\tilde{\nu}}$), respectively, $N_{t,IR}$ is the number of infrared time samples and $N_{\tilde{\nu}}$ is the number of wave numbers in the reaction spectrum. The matrix C_{Calc} (dimension $N_{t,IR} \times N_C$, where N_C is the number of chemical components in the reaction model) contains the concentration time profiles of the eight components calculated by numerical integration of the reaction model (Eq. (1)). Matrix E contains the eight unknown pure component spectra (dimension $N_C \times N_{\tilde{\nu}}$). E_n is the nth column vector of matrix E at the nth wave number.

As shown by Eqs. (6)–(9), the estimation of the matrix of pure component spectra E is carried out by applying a linear least-squares minimization at each wave number. As a constrained algorithm is used, measured pure spectra could be included into the estimation of E in order to circumvent a possible rank deficiency of the matrix C_{Calc}. However, as will be shown later, the rank deficiency does not influence the estimation of the desired reaction model parameters ($k_{1,2}\Delta_r H_{1,2}$, $E_{A,1,2}$). Thus, the inclusion of separately measured pure spectra is only required if the pure spectra of the reaction components were of further interest. It should be mentioned that the evaluation of the infrared data by Eqs. (6)–(9) is a straightforward approach, which allows a direct inclusion of bounds for the estimated pure component spectra. For example, the reduction of linear spectral unknowns described by Maeder and Zuberbühler (1990) was not implemented as the calculation time is rather dominated by the numerical integration of the reaction model.

If several experiments are carried out they can be evaluated in one single step by concatenating the measured data to an augmented q_{Data} vector and A_{Data} matrix. If several experiments are evaluated at the same time, unique reaction enthalpies $\Delta_r H_1$ and $\Delta_r H_2$ can be used for all experiments. The nonlinear optimization (Eq. (3)) is repeated 10 times using random start values in a user-defined range. The nonlinear optimization algorithm uses the same range as boundary conditions for the model parameters.

The crucial task of the Combined Evaluation Algorithm however is the determination of S_{IR}, S_q, $\Delta q_{\min}$ as well as $\Delta A_{\min}$ in order to calculate the combined objective function according to Eq. (3). For the epoxidation reaction described above, the two objectives are to minimize $\Delta q(k_1, k_2, E_{A,1}, E_{A,2})$ ((W^2), Eq. (4)) as well as $\Delta A(k_1, k_2, E_{A,1}, E_{A,2})$ ([-], Eq. (6)) by varying the rate constants as well as the activation energies.

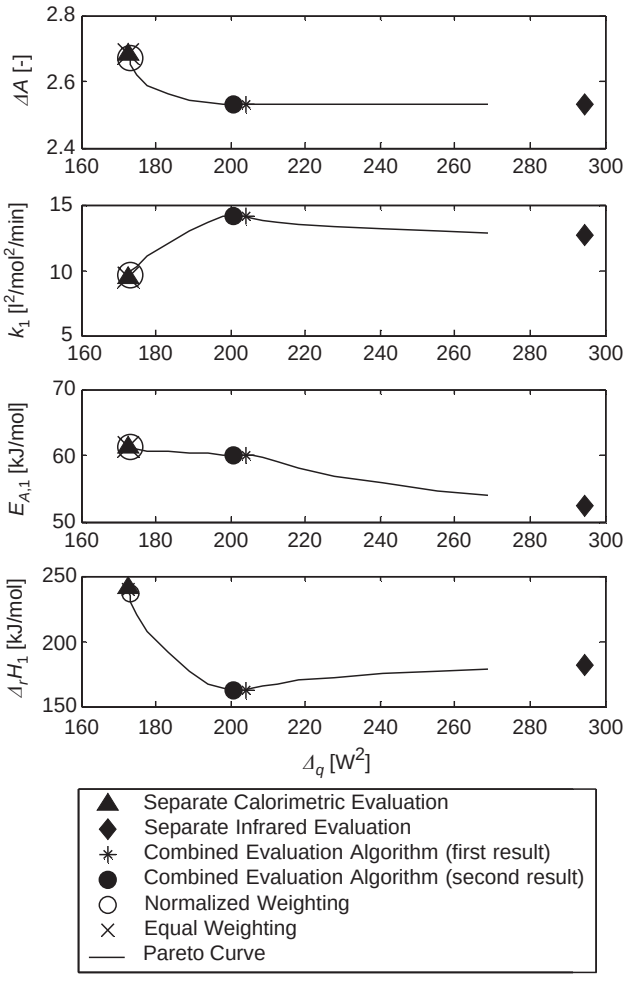

Fig. 3. Comparison of different separate and combined evaluations based on Eq. (3) using all experiments conducted for the epoxidation reaction given in Fig. 1. Only three of the total six reaction model parameters are shown. However, k_2, $E_{A,2}$ as well as $\Delta_r H_2$ show a similar behavior. The value of k_1 at 30 °C is shown.

For a meaningful combined evaluation, these two objective functions have to be scaled or weighted and then totalized. If no scaling would be applied, the evaluation would always be dominated by one of the two objective functions. Generally, the determined model parameters ($k_1, k_2, E_{A,1}, E_{A,2}$) will thus depend on the selected weighting or scaling factors. This behaviour is demonstrated in Fig. 3 using the evaluation of all experiments conducted for the epoxidation reaction example investigated in this study.

The first plot shows the Pareto curve (solid line) of the two objective functions (Δq and ΔA) that have to be minimized during the combined optimization. The calculation was carried out according to Eq. (3) by setting $S_{IR} = 0 \rightarrow$

∞, $S_q = 1$, and $\Delta A_{\min} = \Delta q_{\min} = 0$. In the lower three plots, the corresponding reaction model parameters (only k_1, $E_{A,1}$ and $\Delta_r H_1$) are shown. As mentioned above, the reaction model parameters depend significantly on the scaling factor S_{IR} and the crucial task of choosing an appropriate S_{IR} is left to the user.

The end points of the Pareto diagram can also be obtained by Eq. (3): (i) conducting a *Separate Calorimetric Evaluation* by setting $S_{IR} = \Delta q_{\min} = \Delta A_{\min} = 0$ and $S_q = 1$, and (ii) conducting a *Separate Infrared Evaluation* by setting $S_q = \Delta q_{\min} = \Delta A_{\min} = 0$ and $S_{IR} = 1$. These results are also shown in Fig. 3. For the chosen example, the variables $\Delta q_{\min}$ as well as $\Delta A_{\min}$ can now be determined: $\Delta q_{\min} = 173\ \mathrm{W}^2$, $\Delta A_{\min} = 2.53$. The corresponding reaction model parameters determined during these evaluations are shown in the lower three plots. The results in Fig. 3 show that the reaction model parameters on the Pareto curve can lay outside of the range given by the separate evaluations.

The results of a first attempt to combine the two objective functions according to Eq. (3) by setting $S_{IR} = S_q = 1$ and $\Delta q_{\min} = \Delta A_{\min} = 0$ are also shown in Fig. 3 where it is referred to as *Equal Weighting*. The results are dominated by the calorimetric measurements and thus correspond to the Separate Calorimetric Evaluation. For this example, no combination of the two objectives is achieved with this approach.

A standard attempt to combine the two objective functions could be to normalize the two data sets. This can be achieved if q_{Data}, q_{Calc}, A_{Data} as well as A_{Calc} in Eqs. (4)–(8) are replaced by their normalized equivalents:

$$q_{\mathrm{Data,\ norm}} = \frac{q_{\mathrm{Data}} - \min(q_{\mathrm{Data}})}{\max(q_{\mathrm{Data}}) - \min(q_{\mathrm{Data}})}$$
$$q_{\mathrm{calc,\ norm}} = \frac{q_{\mathrm{calc}} - \min(q_{\mathrm{Data}})}{\max(q_{\mathrm{Data}}) - \min(q_{\mathrm{Data}})} \tag{10}$$

$$A_{\mathrm{Data,\ norm}} = \frac{A_{\mathrm{Data}} - \min(A_{\mathrm{Data}})}{\max(A_{\mathrm{Data}}) - \min(A_{\mathrm{Data}})}$$
$$A_{\mathrm{calc,\ norm}} = \frac{A_{\mathrm{calc}} - \min(A_{\mathrm{Data}})}{\max(A_{\mathrm{Data}}) - \min(A_{\mathrm{Data}})} \tag{11}$$

The combined evaluation according to Eq. (3) can now be carried out by setting $S_{IR} = 1/(N_{t,IR} N_{\tilde{\nu}})$, $S_q = 1/N_{t,q}$ and $\Delta q_{\min} = \Delta A_{\min} = 0$. The corresponding results are shown in Fig. 3 and are referred to as *Normalized Weighting*. These results are again dominated by the calorimetric measurements and thus correspond to the Separate Calorimetric Evaluation. For this example, no combination of the two objectives is achieved with this approach.

For the Combined Evaluation Algorithm, an automatic procedure was therefore developed that delivers the required scaling factors S_{IR} and S_q in Eq. (3). In a first step, a Separate Calorimetric Evaluation (Eq. (12)) and a Separate Infrared Evaluation (Eq. (13)) are carried out in order to determine the minimal calorimetric error $\Delta q_{\min}(\mathrm{W}^2)$ as well as the minimal infrared error $\Delta A_{\min}[\text{-}]$:

$$\Delta q_{\min} = \min_{k_1,k_2,E_{A,1},E_{A,2}} [\Delta q(k_1, k_2, E_{A,1}, E_{A,2}) \rightarrow \text{estimated parameters} : \theta_{q,1..N_P} \tag{12}$$

$$\Delta A_{\min} = \min_{k_1,k_2,E_{A,1},E_{A,2}} [\Delta A(k_1, k_2, E_{A,1}, E_{A,2})] \rightarrow \text{estimated parameters} : \theta_{IR,1..N_P} \tag{13}$$

where N_P is the number of model parameters (for this example equal to four: k_1, k_2, $E_{A,1}$, and $E_{A,2} \hat{=} \theta_{1..Np}$) to be determined. The method then calculates the scaling factors S_q and S_{IR} within three steps, starting with a sensitivity analysis of the single objective functions Δq and ΔA with respect to the model parameters. The sensitivity is calculated by inverting the average deviations of Δq and ΔA from their minimal values $\Delta q_{\min}$ and $\Delta A_{\min}$ caused by a change of all the model parameters (positive as well as negative deviation):

$$S_{q,1} = \frac{2N_P}{\sum_{i=1}^{N_P} |\Delta q(\theta_{q,i} + \Delta\theta_i) - \Delta q_{\min}| + \sum_{i=1}^{N_P} |\Delta q(\theta_{q,i} - \Delta\theta_i) - \Delta q_{\min}|} \tag{14}$$

$$S_{IR,1} = \frac{2N_P}{\sum_{i=1}^{N_P} |\Delta q(\theta_{IR,i} + \Delta\theta_i) - \Delta A_{\min}| + \sum_{i=1}^{N_P} |\Delta A(\theta_{IR,i} - \Delta\theta_i) - \Delta A_{\min}|} \tag{15}$$

where $\Delta\theta_i$ is defined as follows:

$$\Delta\theta_i = \theta_{q,i} - \theta_{IR,i} \tag{16}$$

In a second step, a combined optimization is carried out based on Eq. (3) (using $S_{q,1}$ and $S_{IR,1}$ as S_q and S_{IR}). The results of the first iteration of the Combined Evaluation Algorithm are shown in Fig. 3. In a third step, the calculation of the scaling factors (Eqs. (14) and (15)) is repeated using the model parameters from the preceding combined optimization instead of $\theta_{q,1..Np}$ and $\theta_{IR,1..Np}$ obtained from Eqs. (12) and (13). Finally, the combined optimization (Eq. (3)) is repeated using the updated scaling factors. The results of the second iteration of the Combined Evaluation Algorithm are shown in Fig. 3. The difference to the first combined optimization is rather small. Therefore, the iterative adaptation of the scaling factors S_{IR} and S_q was not continued although in principle this is possible.

The influence of the calorimetric and infrared error functions on the combined objective function (Eq. (3)) is thus equalized in two ways: (i) by subtraction of $\Delta q_{\min}$ and $\Delta A_{\min}$ the absolute values of the two error functions Δq and ΔA are equalized, and (ii) by applying the automatically determined scaling factors S_q and S_{IR}, the change of $\Delta q - \Delta q_{\min}$ caused by a change of the reaction model parameters (k_1, k_2, $E_{A,1}$ or $E_{A,2}$) is similar to the change of $\Delta A - \Delta A_{\min}$. The applied scaling principle will thus automatically equalize the

influence of the two measured data sets (calorimetric and infrared data) on the determined reaction model parameters.

The time consuming part of the evaluation algorithm (Eqs. (4) and (9), including the numerical integration of the reaction model) is written in C and included into Matlab® as a Dynamic Link Library. The outer optimization loop is running in Matlab® using the *fmincon* function for the non-linear optimization (Matlab Optimization Toolbox). For a more detailed description of the presented calculation method refer to Zogg et al. (2004a) or Zogg (2003).

3. Experimental section

The prototype reaction calorimeter (Zogg, 2003; Zogg et al., 2003) used for all reaction experiments of this work has a sample volume of 25–45 ml, is combined with an IR-ATR probe and runs at strictly isothermal operation conditions. The ATR probe (Axiom, DMD 260) is connected to a Bruker FTIR spectrometer (Equinox 55). The spectra were recorded with a resolution of 4 cm^{-1} and a sampling time of 11.5 s (15 samples). The spectral region between 1800 and 2400 cm^{-1} was cut off by the diamond of the ATR sensing head.

3.1. Experimental procedure for the epoxidation of 2,5-di-tert-butyl-1,4-benzoquinone

After the reactor was cleaned, evacuated and purged with N_2, 1.29 g of 2,5-di-tert-butyl-1,4-benzoquinone (Aldrich, 5.85 mmol) were added. Care was taken that the benzoquinone did not touch the ATR Sensor. After having reached the desired jacket temperature, a reference background spectrum for the infrared measurement was taken. Then, 19.2 ml Dioxan (Baker), 8 ml EtOH (Baker), and 8 ml tert-butyl hydroperoxide (Aldrich, 70% solution in water, 58.5 mmol) were added subsequently. The stirrer was turned on to 400 rpm and the desired reaction temperature was set. After degassing the solution for 3 min with N_2, 0.8 ml of Triton B (Fluka, 40% in methanol, 1.78 mmol) were dosed within 24 s into the closed reactor to start the reaction. This experiment was carried out four times at 17 °C and three times at 24, 30 and 36 °C. The reaction conditions were chosen similar to the ones reported by Mayes et al. (1992). The infrared spectra were evaluated in the range of 740 ∼ 860, 1150 ∼ 1450, and 1580 ∼ 1780 cm^{-1} (see Fig. 4). The baseline drift of the spectrometer was corrected by subtracting an average absorbance time profile at 712, 810, 1310, and 1550 cm^{-1} from the raw reaction spectra. The reaction spectra of all experiments were then concatenated to a single A_{Data} matrix (Eq. (7)). Similarly, the calorimetric data was concatenated to a single q_{Data} vector (Eq. (4)).

Three additional experiments at 30 °C were carried out using only 5 ml tert-butyl hydroperoxide (Aldrich, 70% solution in water, 36.4 mmol) instead of 8 ml. The measured reaction data of all six experiments at 30 °C were then concatenated to a second A_{Data} matrix and q_{Data} vector. The experimental procedure is described in further detail in Zogg (2003).

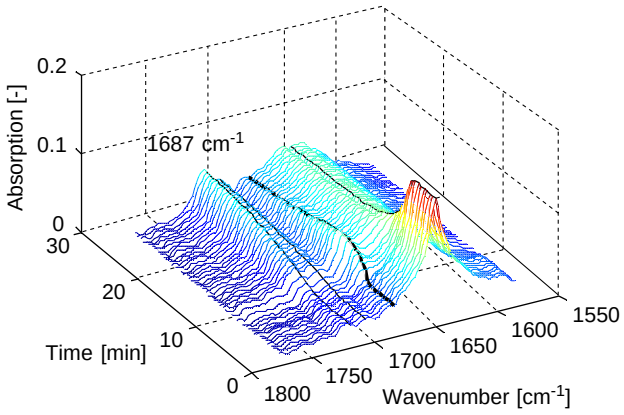

Fig. 4. Epoxidation of 2,5-di-tert-butyl-1,4-benzoquinone: one part of the infrared spectrum recorded as a function of time at 17 °C. The peak at 1687 cm^{-1} is indicated with a fat line and is used for illustration purposes in Fig. 5.

3.2. Reference data

The epoxidation reaction was chosen because it was one of the few consecutive reaction examples for which several empirical kinetic reference data are available (Hairfield et al., 1985; Mayes et al., 1992; Bijlsma et al., 1998). The empirical kinetic model used by all authors can be written as follows (according to Fig. 1):

$$r_1 = k_1^+ c_{\text{Educt}} \quad r_2 = k_2^+ c_{\text{Mono Epoxide}} \tag{17}$$

where k_1^+ and k_2^+ (l/mol/s) are the rate constants of the first and second epoxidation step. Unfortunately, different concentrations of the catalyst, 2,5-di-tert-butyl-1,4-benzoquinone, and tert-butyl hydroperoxide were used in the different studies. Therefore, the reported values had to be transformed, assuming first-order behavior in the catalyst and hydroperoxide concentration (for further details refer to Zogg (2003)):

$$k_1 = k_1^+ / c_{\text{cat},0} / c_{\text{Hydroperoxide},0}$$
$$k_2 = k_2^+ / c_{\text{cat},0} / c_{\text{Hydroperoxide},0} \tag{18}$$

where $c_{\text{cat},0}$ and $c_{\text{Hydroperoxide},0}$ are the initial catalyst and hydroperoxide concentration (mol/l). The rate constants k_1 and k_2 ($l^2/mol^2/s$) can now be compared between the different references and to the rate constants estimated in this study as will be done below.

No measured reaction enthalpies for the epoxidation reaction were found in literature. Based on standard heats of formation of different saturated olefins (NIST, 2003; Dowd et al., 1991), as well as an indirectly determined epoxidation enthalpy of a benzoquinone system (Flowers et al., 1993), the reaction enthalpy of a single epoxidation step was calculated to be in the range of −153 (benzoquinone system) to

−212 kJ/mol (1-Butene). For further details, refer to Zogg (2003). However, no indications for a different epoxidation enthalpy of the first and second epoxidation step were found. Therefore, semi-empirical quantum mechanical calculations were carried out to estimate the heat of formation of the involved compounds. CAChe (2002) and HyperChem (2002) as well as four different Hamiltonians (AM1, PM3, PM5, MNDO) were used. In most of the calculations, the first epoxidation step (compare to Fig. 1) turned out to be slightly more exothermal than the second step. It should be noted that the standard deviation of the average values obtained from these calculations are higher than the difference between $\Delta_r H_1$ and $\Delta_r H_2$. Below, these values will be compared to those determined from the Combined Evaluation Algorithm.

4. Results and discussion

The reaction measurements were evaluated in different ways in order to demonstrate the performance of the new Combined Evaluation Algorithm. The different evaluations are summarized in Table 1, a detailed discussion will be given below. All three evaluation approaches Separate Calorimetric Evaluation, Separate Infrared Evaluation, and Combined Evaluation Algorithm identify the same reaction parameters. However, it should be noted that the reaction enthalpies determined by the Separate Infrared Evaluation are determined in two steps: (i) identification of the kinetic reaction model parameters based on the infrared data only (Eq. (13)); (ii) using these identified parameters the reaction enthalpies can be subsequently determined by applying Eq. (4). In the following, the results obtained for the different reaction models and physical constraints will be discussed.

4.1. Case study A: $\Delta_r H_1$ is allowed to deviate from $\Delta_r H_2$

In addition to the measurement data (4, 3, 3, and 3 measurements at 17, 24, 30 and 36 °C, respectively, identical concentrations) and the reaction model described by Eq. (1), bounds for the unknown reaction parameters are required in order to apply the Combined Evaluation Algorithm.

As several isothermal reaction measurements at different temperatures are evaluated at the same time, the rate constants k_1 and k_2 in Eq. (1) were expressed according to Eq. (2). Thus for the unknown reaction parameters k_1 and k_2 (at $T_{\text{ref}} = 25\,^{\circ}\text{C}$), a range, of 0–38 ($\text{l}^2/\text{mol}^2/\text{min}$) was chosen, and for the unknown activation energies $E_{A,1}$ and $E_{A,2}$ a range of 10–150 (kJ/mol). A total of 10 sets of random start values were used for these four nonlinear reaction model parameters. Additionally, two reaction enthalpies $\Delta_r H_1$ and $\Delta_r H_2$ had to be identified inside the range of 0 to −1000 kJ/mol. The same reaction enthalpies were used for all temperatures. Finally, feasible bounds for the eight pure component spectra (educt, hydroperoxide, mono Epoxide, di Epoxide, alcohol, methanol, solvent, Triton B) had to be specified. As no measured pure spectra were used, all absorption coefficients at all wave numbers and for all components were constrained in the range of 0–5. For each temperature, a new set of pure component spectra (matrix E) was identified, otherwise it was not possible to describe the measurement data accurately. Based on this input data, the evaluation of the measurements was carried out for the three evaluation types:

4.1.1. Evaluation A.1: Combined Evaluation Algorithm

The developed scaling procedure automatically determined the scaling factors $S_{IR} = 30$ and $S_q = 0.009$ (W^{-2}). Out of 10 random start value sets, eight resulted in the same optimum, indicating a robust identification. The quality of the model fit is shown in Fig. 5 (only measurements at 17 and 30 °C are shown). For illustration purposes, only one wave number at 1687 cm^{-1} is shown in the two lower plots (compare to Fig. 4); however, all wave numbers were evaluated and peak overlapping was allowed. It can be concluded that the calorimetric as well as the infrared data were successfully modeled by the specified reaction model (Eq. (1), $\Delta q = 201\ \text{W}^2$, $\Delta A = 2.529$) and the identified reaction model parameters (k_1, k_2, $E_{A,1}$, $E_{A,2}$), which are listed in Table 3. In Table 2, the identified reaction enthalpies ($\Delta_r H_1$ and $\Delta_r H_2$) are listed. They are compared to the sum of $\Delta_r H_1$ and $\Delta_r H_2 (= \Sigma \Delta_r H_i)$ determined by integration of the calorimetric signal, to literature references based on standard heats of formations, and to the results of the semi-empirical calculations.

The complete calculation time using an Intel Pentium M, 1.4 MHz, 512 MB RAM is 2.6 h. The calculation comprises the following:

- Separate calorimetric as well as infrared evaluation in order to determine $\Delta q_{\min}$ as well as $\Delta A_{\min}$ (Eqs. (12) and (13)).
- Two iterative applications of the Combined Evaluation Algorithm in order to determine the appropriate scaling factors S_{IR} as well as S_q.
- All four evaluations were carried out 10 times using random start values for the reaction model parameters (in the defined range given above).
- A total of 13 experiments were evaluated at the same time—including numerical integration of the reaction model (Eq. (1)) for each experiment.

The average calculation time for one experiment using only one start value is therefore only 12 min.

4.1.2. Evaluation A.2: Separate Calorimetric Evaluation

Out of 10 random start value sets, all resulted in the same optimum (see Table 2 and 3), indicating a very robust identification. The model fit quality was similar to evaluation A.1 ($\Delta q = \Delta q_{\min} = 173\ W^2$, $\Delta A = 2.685$).

Table 1
Overview on the different evaluations carried out and the different measurement data used

	Case study A	Case study B	Case study C
Combined Evaluation Algorithm Eq. (3)	A.1	B.1	C.1
Separate Calorimetric Evaluation Eq. (12)	A.2	B.2	C.2
Separate Infrared Evaluation Eqs. (4) and (13)	A.3	B.3	C.3
Measurement data at 17, 24, 30, and 36 °C with equal concentrations	✔	✔	—
Measurement data at 30 °C with different concentrations	—	—	✔
Special physical constraint	—	$\Delta_r H_1 = \Delta_r H_2$	—
Identified reaction parameters	k_1, k_2 $E_{A,1}$, $E_{A,2}$ $\Delta_r H_1$, $\Delta_r H_2$	k_1, k_2 $E_{A,1}$, $E_{A,2}$ $\Delta_r H$	k_1, k_2 $\mathrm{ord}_{\mathrm{Cat}}$, $\mathrm{ord}_{\mathrm{HP}}$ $\Delta_r H_1$, $\Delta_r H_2$

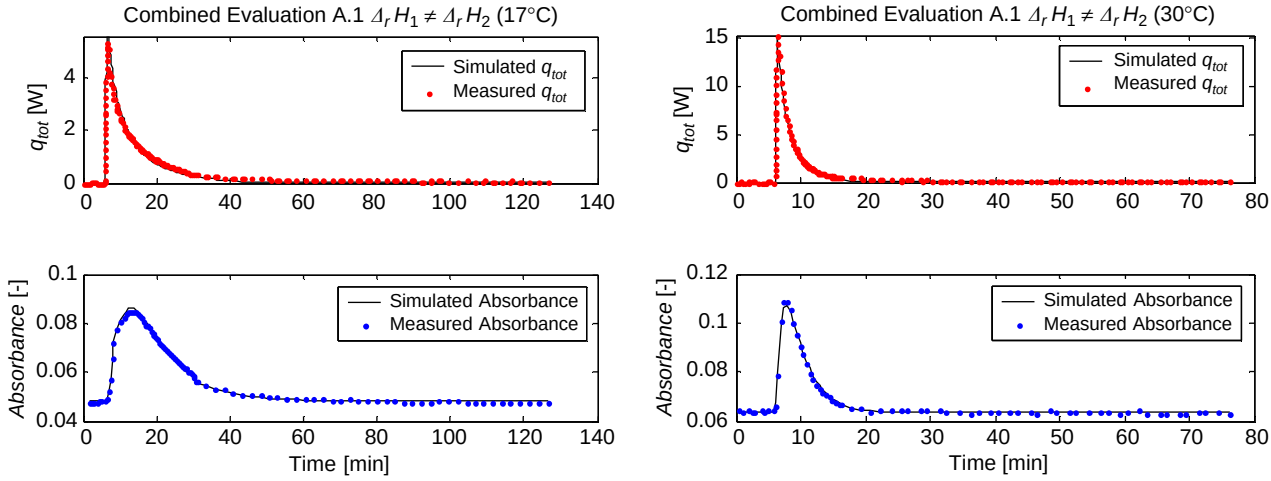

Fig. 5. Evaluation A.1, epoxidation of 2,5-di-tert-butyl-1,4-benzoquinone using the Combined Evaluation Algorithm. All experiments at all temperatures were evaluated simultaneously. A mean value of all reaction experiments at each temperature is shown. Only one wave number (1687 cm^{-1}) of the reaction spectrum is shown in the lower plots.

Table 2
Results of the different evaluations A.1–A.3 and B.1–B.3: Identified reaction enthalpies $\Delta_r H_1$ and $\Delta_r H$ ($\Sigma\Delta_r H_i = \Delta_r H_1 + \Delta_r H_2$). The reaction model is described by Eq. (1)

$\Sigma\Delta_r H_i$, (kJ/mol)	Integration of q_{tot}[a]	17 °C -440 ± 50	24 °C -440 ± 20	30 °C -480 ± 30	36 °C -440 ± 10
	Literature[b]	-307–-424			
$\Delta_r H_1$, $\Delta_r H_2$, (kJ/mol) equal for all temperatures	Semi empirical[c]		$\Delta_r H_1 = -140 \pm 20$	$\Delta_r H_2 = -130 \pm 10$	$\Sigma\Delta_r H_i = -270$
	Combined Evaluation Algorithm (A.1)		$\Delta_r H_1 = -160$	$\Delta_r H_2 = -200$	$\Sigma\Delta_r H_i = -360$
	Separate Calorimetric Evaluation (A.2)		$\Delta_r H_1 = -240$	$\Delta_r H_2 = -150$	$\Sigma\Delta_r H_i = -390$
	Separate Infrared Evaluation (A.3)		$\Delta_r H_1 = -180$	$\Delta_r H_2 = -170$	$\Sigma\Delta_r H_i = -350$
	Combined Evaluation Algorithm (B.1)		$\Delta_r H_1 = -180$	$\Delta_r H_2 = -180$	$\Sigma\Delta_r H_i = -360$
	Separate Calorimetric Evaluation (B.2)		$\Delta_r H_1 = -190$	$\Delta_r H_2 = -190$	$\Sigma\Delta_r H_i = -380$
	Separate Infrared Evaluation (B.3)		$\Delta_r H_1 = -180$	$\Delta_r H_2 = -180$	$\Sigma\Delta_r H_i = -360$

[a]Direct integration of the calorimetric data without using a reaction model.
[b]Calculation based on standard heats of formation (see text for further details).
[c]Determined by semi-empirical quantum mechanical calculations (see text for further details).

The complete calculation time using an Intel Pentium M, 1.4 MHz, 512 MB RAM is 36 min. The average calculation time for one experiment using only one start value is therefore 2.7 min.

4.1.3. Evaluation A.3: Separate Infrared Evaluation

Out of 10 random start value sets, six resulted in the same optimum, indicating a medium robust identification The results are also given in Tables 2 and 3. The model

Table 3
Results of the different evaluations A.1–A.3 and B.1–B.3: Identified reaction model parameters k_1, k_2, $E_{A,1}$, $E_{A,2}$. The rate constants k_1 and k_2 were identified at 30 °C. Using the identified activation energies $E_{A,1}$ and $E_{A,2}$, the rate constants at 17, 24, and 36 °C were calculated by Eq. (2). The reaction model is described by Eq. (1)

	k_1, k_2 (l^2/mol^2/min)				$E_{A,1}$, $E_{A,2}$ (kJ/mol)
	17 °C	24 °C	30 °C	36 °C	
Literature[a]	5 ± 1	—	17 ± 1	—	75
	1 ± 1		4 ± 3		72
Combined Evaluation Algorithm (A.1)	4.9	8.8	14.2	22.5	60
	1.2	2.4	4.2	7.3	70
Separate Calorimetric Evaluation (A.2)	3.2	5.8	9.4	15.1	61
	0.6	1.2	2.1	3.8	76
Separate Infrared Evaluation (A.3)	5.0	8.3	12.6	18.9	53
	1.3	2.6	4.7	8.2	73
Combined Evaluation Algorithm (B.1)	4.5	8.1	13.0	20.7	60
	1.3	2.5	4.4	7.3	69
Separate Calorimetric Evaluation (B.2)	4.2	7.6	12.3	19.6	60
	0.8	1.8	3.3	6.0	73
Separate Infrared Evaluation (B.3)	5.0	8.3	12.6	18.9	53
	1.3	2.6	4.7	8.2	73

[a]Transformed and averaged literature references (for details, see Zogg (2003)).

fit quality was similar to evaluation A.1 ($\Delta q = 294$ W^2, $\Delta A = \Delta A_{\min} = 2.528$).

The complete calculation time using an Intel Pentium M, 1.4 MHz, 512 MB RAM is 48 min. The average calculation time for one experiment using only one start value is therefore 3.7 min.

When comparing the three sets of results obtained for the different evaluation types (Tables 2 and 3) it can be concluded that the separate evaluations of the calorimetric and infrared data did not result in the same reaction parameters. It is therefore essential to apply the Combined Evaluation Algorithm in order to obtain a unique set of reaction parameters that represents an optimal solution for all measured data. It should be noted that some of the reaction parameters ($\Delta_r H_1$, $\Delta_r H_2$, k_1, $E_{A,2}$) determined by the Combined Evaluation Algorithm (A.1) are outside the range defined by the separate evaluations (A.2, A.3). It would therefore be unreasonable to simply average the identified reaction parameters of the separate evaluations (A.2, A.3) in order to determine a unique set of reaction parameters.

A comparison of the different identified reaction enthalpies reveals that the calorimetric evaluation (A.2) shows a large difference between $\Delta_r H_1$ and $\Delta_r H_2$ (90 kJ/mol), whereas $\Delta_r H_1$ and $\Delta_r H_2$ identified by the infrared evaluation (A.3) only differ by 10 kJ/mol. The Combined Evaluation Algorithm (difference 40 kJ/mol) lies in-between. However, considering the small difference predicted by the semi-empirical quantum mechanical calculations (see Table 2), in particular, the results of the calorimetric evaluation become unreasonable.

All three evaluations (A.1, A.2, A.3) identified $E_{A,1}$ to be smaller than $E_{A,2}$. Such a difference was not found by the literature references. However, it should be noted that some inconsistencies were found in the literature values (for a further analysis refer to Zogg (2003)). The difference of $E_{A,1}$ and $E_{A,2}$ suggested by the infrared evaluation is rather large (20 kJ/mol), whereas the results of the Combined Evaluation Algorithm are most reasonable from the point of mechanistic considerations. Comparing the determined rate constants it is concluded that the results of the Combined Evaluation Algorithm (A.1) agree well with the literature references.

Since the rank of the calculated concentration matrix C_{Calc} (obtained by integration of Eq. (1)) equals five, the eight identified pure component spectra in matrix E (Eq. (9)) were not reasonable (linear dependencies) as the concentration time profiles in C_{Calc} are linearly dependent. However, it is important to note that the identification of the required reaction parameters is not influenced by these linear dependences as they do not affect ΔA in Eq. (3). For simpler reaction systems, it is even possible to identify the pure component spectra. This was shown based on the hydrolysis of acetic anhydride in Zogg et al. (2004a) and Zogg (2003). For a more complex reaction example, such as the one shown here, the determination of the pure component spectra could be achieved by the inclusion of bounds for some of the pure component spectra. This is straightforward as for the linear least-squares optimization in Eq. (7) a constraint algorithm is used. However, the identification of pure component spectra is not the topic of this work.

4.2. Case study B: Additional constraint: $\Delta_r H_1 = \Delta_r H_2$

Based on the discussion of the identified $\Delta_r H_1$ and $\Delta_r H_2$ by case study A and the results of the semi-empirical quantum mechanical calculations (see above), another evaluation was carried out using the additional constraint $\Delta_r H_1 = \Delta_r H_2$. Again the evaluation was carried out three different times:

4.2.1. Evaluation B.1: Combined Evaluation Algorithm

The developed scaling procedure automatically determined the scaling factors $S_{IR} = 111$ and $S_q = 0.017$ (W^{-2}). Out of 10 random start value sets, all resulted in the same optimum, indicating a very robust identification. The quality of the model fit is slightly worse compared to evaluation A but still satisfying and optically identical to Fig. 5 ($\Delta q = 210$ W^2, $\Delta A = 2.529$). The identified reaction parameters are listed in Tables 2 and 3.

4.2.2. Evaluation B.2: Separate Calorimetric Evaluation

Out of 10 random start value sets, all resulted in the same optimum (see Tables 2 and 3), indicating a very robust identification. The model fit quality was similar to evaluation B.1 ($\Delta q = \Delta q_{\min} = 183$ W^2, $\Delta A = 2.571$).

4.2.3. Evaluation B.3: Separate Infrared Evaluation

Out of 10 random start value sets, six resulted in the same optimum, indicating a medium robust identification. The identified reaction model parameters are given in Table 3. They are identical to evaluation A.3 as the additional constraint has no influence on Eqs. (6)–(9). In Table 2, the identified reaction enthalpies ($\Delta_r H_1$ and $\Delta_r H_2$) are listed. They are influenced by the additional constraint and thus no more identical to evaluation A.3. The model fit quality was similar to evaluation B.1 ($\Delta q = 305$ W^2, $\Delta A = \Delta A_{\min} = 2.528$).

When comparing the results of this case study to the results of case study A (see Tables 2, 3), it can be concluded that the Separate Calorimetric Evaluations (A.2, B.2) significantly differ in most reaction model parameters ($\Delta_r H_1$, $\Delta_r H_2$, k_1, k_2), whereas the Separate Infrared Evaluations (A.3, B.3) only show slightly different reaction enthalpies. The results obtained with the Combined Evaluation Algorithm (A.1, B.1) significantly differ in the identified reaction enthalpies. The reaction model parameters are only slightly affected. The identified activation energies $E_{A,1}$ and $E_{A,2}$ are similar to case study A and thus the comments are equal.

As compared to case study A, the separate evaluation of the calorimetric (B.2) and infrared data (B.3) differ less (similar $\Delta_r H_1$, $\Delta_r H_2$, k_1, $E_{A,1}$, $E_{A,2}$, different k_2), but it is still essential to apply the Combined Evaluation Algorithm in order to obtain a unique set of reaction parameters. Similar to case study A, some of the reaction parameters (k_1, $E_{A,2}$) determined by the Combined Evaluation Algorithm (B.1) are outside of the range defined by the separate evaluations (B.2, B.3).

4.3. Case Study C: Different reaction model

As mentioned above, three additional experiments at 30 °C were carried out using less hydroperoxide. They were evaluated together with the three standard measurements at 30 °C. Thus, the dependency of the reaction kinetics on the hydroperoxide concentration can be analyzed. Therefore, the definitions of the reaction rates r_1 and r_2 in Eq. (1) were replaced by the following modified empirical reaction model:

$$r_1(t, k_1', \mathrm{ord_{Cat}}, \mathrm{ord_{HP}}) = k_1' \frac{n_{\mathrm{Educt}}(t)}{V_r(t)} \left[\frac{n_{\mathrm{Triton\ B}}(t)}{V_r(t)}\right]^{\mathrm{ord_{Cat}}} \times \left[\frac{n_{\mathrm{Hydroperoxide}}(t)}{V_r(t)}\right]^{\mathrm{ord_{HP}}}$$

$$r_2(t, k_2', \mathrm{ord_{Cat}}, \mathrm{ord_{HP}}) = k_2' \frac{n_{\mathrm{Mono\ Epoxide}}}{V_r(t)} \left[\frac{n_{\mathrm{Triton\ B}}(t)}{V_r(t)}\right]^{\mathrm{ord_{Cat}}} \times \left[\frac{n_{\mathrm{Hydroperoxide}}(t)}{V_r(t)}\right]^{\mathrm{ord_{HP}}} \quad (19)$$

where k_1' and k_2' are the unknown rate constants of the two epoxidation steps. They were identified within the range 0–1 $((\mathrm{l/mol})^{(\mathrm{ord_{Cat}}+\mathrm{ord_{HP}})}/\mathrm{s})$. As only experiments at 30 °C were evaluated, no activation energies were identified. The reaction orders $\mathrm{ord_{Cat}}$ and $\mathrm{ord_{HP}}$ [-] of the catalyst and hydroperoxide concentration were identified within the bounds of 0–3 and −3 to 3, respectively. Similar to case study A, the two reaction enthalpies $\Delta_r H_1$ and $\Delta_r H_2$ were identified within the bounds of 0 to −1000 kJ/mol and all absorption coefficients at all wave numbers and for all components were constrained in the range of 0 to 5. Based on this input data, the evaluation of the measurements was carried out in three different ways:

4.3.1. Evaluation C.1: Combined Evaluation Algorithm

The developed scaling procedure automatically determined the scaling factors $S_{IR} = 33$ and $S_q = 0.009$ (W^{-2}). Out of 10 random start value sets, all resulted in the same optimum, indicating a very robust identification. The calorimetric as well as the infrared data of all the six experiments were successfully modeled by the specified reaction model (Eq. (19), $q = 58$ W^2, $\Delta A = 0.284$) and the identified reaction model parameters. The identified reaction model parameters (k_1', k_2', $\mathrm{ord_{Cat}}$, $\mathrm{ord_{HP}}$) as well as the reaction enthalpies ($\Delta_r H_1$ and $\Delta_r H_2$) are listed in Table 4.

4.3.2. Evaluation C.2: Separate Calorimetric Evaluation

Out of 10 random start value sets, all resulted in the same optimum, indicating a very robust identification (see Table 4). The model fit quality was similar to evaluation C.1 ($\Delta q = \Delta q_{\min} = 45$ W^2, $\Delta A = 0.326$).

4.3.3. Evaluation C.3: Separate Infrared Evaluation

Out of 10 random start value sets, only one resulted in the optimum, indicating a low robustness of identification (see Table 4). The model fit quality was similar to evaluation C.1 ($\Delta q = 104$ W^2, $\Delta A = \Delta A_{\min} = 0.282$).

Similar to case studies A and B, Table 4 shows that the separate calorimetric and infrared evaluations did not result

Table 4
Results of the evaluations C.1–C.3: Identified reaction model (k_1', k_2', ord_{Cat}, ord_{HP}) and thermodynamic reaction parameters ($\Delta_r H_1$, $\Delta_r H_2$) based on six measurements at 30 °C at different hydroperoxide concentrations. A modified reaction model (Eq. (19)) was applied

30 °C	*Combined Evaluation Algorithm* (C.1)	*Separate Calorimetric Evaluation* (C.2)	*Separate Infrared Evaluation* (C.3)
$\Delta_r H_1$, $\Delta_r H_2$, $\Sigma\Delta_r H_i$ (kJ/mol)	−180	−240	−200
	−180	−140	−140
	−360[a]	−380[a]	−340[a]
k_1', k_2' $((l/\text{mol})^{(ord_{Cat}+ord_{HP})}/\text{min})$	36.6	25.2	39.6
	11.1	5.8	15.6
ord_{Cat} (dimensionless)	1.13	1.12	1.20
ord_{HP} (dimensionless)	−0.16	−0.15	−0.18

[a] Sum of $\Delta_r H_1$ and $\Delta_r H_2$.

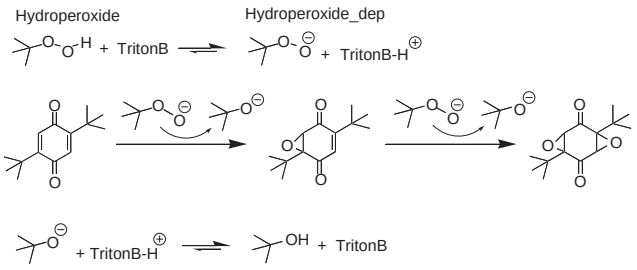

Fig. 6. Conclusion from Evaluation C: hypothesis of a modified reaction model for the epoxidation reaction.

in the same reaction parameters. Application of the Combined Evaluation Algorithm is thus required. Again some of the reaction parameters ($\Delta_r H_1$, $\Delta_r H_2$) determined by the Combined Evaluation Algorithm (C.1) are outside the range defined by the separate evaluations (C.2, C.3). Of all the determined reaction parameters, only the reaction enthalpies are similar to those obtained from case studies A and B. Similar to case study A, the difference of $\Delta_r H_1$ to $\Delta_r H_2$ is maximal and unreasonable for the calorimetric evaluation (100 kJ/mol). The reaction enthalpies determined by the Combined Evaluation Algorithm (C.1) are rather close to the results of case study A and B and are reasonable as they were identified to be equal.

The negative reaction orders determined for the hydroperoxide concentration (ord_{HP}) represent the fact that the reaction experiments carried out using less hydroperoxide proceeded faster compared to the other experiments. However, a negative reaction order does not make sense with the reaction scheme of Fig. 1 and indicates that the empirical reaction model (Eq. (19)) does not accurately describe the epoxidation reaction. A more appropriate guess for a reaction model, which might describe such a situation within the studied concentration region, is given in Fig. 6. In a preliminary equilibrium, the hydroperoxide is deprotonated to produce the active epoxidation reagent. Assuming that these equilibrium reactions are much faster compared to the epoxidation reaction and that at equilibrium the catalyst is nearly completely protonated it might be concluded that the concentration of the active epoxidation reagent (*Hydroperoxide_dep*) increases if the amount of hydroperoxide is decreased due to the total volume decrease (as long as hydroperoxide is in excess). This would explain the observed and identified negative reaction order with respect to the total hydroperoxide concentration. Such a reaction model, which was found based on the results obtained by the new evaluation algorithm, is also supported by mechanistic considerations (Moore, 1967; House, 1972).

5. Conclusions and outlook

The consecutive epoxidation of 2,5-di-tert-butyl-1,4-benzoquinone with tert-butyl hydroperoxide was carried out at different temperatures and initial concentrations of hydroperoxide. The online measured calorimetric (reaction power) and infrared data (reaction spectrum) were evaluated simultaneously, using a new Combined Evaluation Algorithm. The infrared spectra were evaluated without the knowledge of any pure component spectra and overlapping peaks were allowed. The algorithm is able to identify several reaction parameters, such as reaction enthalpies, rate constants, activation energies as well as reaction orders in a single step.

The Combined Evaluation Algorithm was applied to three case studies using different physical constraints and reaction models. In addition, similar evaluations were conducted considering only calorimetric or infrared data. First of all it was shown that the reaction parameters identified by the separate evaluations of the two data sets can differ significantly. It is therefore essential to apply the Combined Evaluation Algorithm in order to obtain a unique set of reaction parameters that represent an optimal solution based on all measured data. The task of performing an appropriate scaling of the calorimetric and infrared data was successfully carried out by the developed automatic scaling principle. It was observed that some of the reaction parameters determined by the Combined Evaluation Algorithm are outside of the solution range defined by the separate evaluations. It would therefore be unreasonable to simply average the reaction parameters determined by the separate evaluations in order to determine a unique set of parameters.

Based on the analysed reaction data, it can further be concluded that the Separate Calorimetric Evaluation was

mathematically robust as for all 10 randomly selected start values the same reaction parameters were identified in all the three case studies. However, the identified reaction parameters were most doubtful as the differences between the identified reaction enthalpies ($\Delta_r H_1$ and $\Delta_r H_2$) are rather large. The separate evaluation of the infrared data generally showed the opposite behavior: the identification of the reaction parameters was mathematically much less robust but reasonable values were obtained, e.g. the differences between the identified reaction enthalpies were small. The Combined Evaluation Algorithm however showed the best overall performance: a mathematically robust identification in all three case studies resulting in reasonable reaction parameters: small differences between $\Delta_r H_1$ and $\Delta_r H_2$ as well as small differences between the identified activation energies ($E_{A,1}$ and $E_{A,2}$). The identification of reaction parameters is thus significantly improved by the application of the Combined Evaluation Algorithm as the two analytical signals complement one another.

Based on the two case studies A and B, it was possible to identify reasonable reaction parameters for identical initial concentrations. The identified reaction parameters of case study B agree well with literature references. By evaluating measurements at different initial hydroperoxide concentrations, it was further shown that the application of the Combined Evaluation Algorithm also supports the identification of a more accurate reaction mechanism. Thus, the proposed analytics combined with the new evaluation signify a major advance in practical applications.

In future work, the concept of simultaneous evaluation of different analytical signals will be extended to the additional measurement of gas uptake or gas production rate during a reaction. Due to the general concept of the presented automatic scaling principle it should not be required to change it for such an application.

References

am Ende, D.J., Clifford, P.J., De Antonis, D.M., Santa Maria, C., Bernek, S.J., 1999. Organic Process Research & Development 3, 319–329.

BatchCAD, Hyprotech: www.hyprotech.com/batchcad.

BatchReactor, ProSim: www.prosim.com.

Bijlsma, S., Louwerse, D.J., Smilde, A.K., 1998. A.I.Ch.E. Journal 44, 2713–2723.

CACHe, 2002. Version 5.0, Fujitsu, CACHe Group: http://www.cachesoftware.com.

ChemCad, Chemstations, Inc.: http://www.chemstations.net.

Dowd, P., Ham, S.W., Geib, S.J., 1991. Journal of the American Chemical Society 113, 7734–7743.

Fillion, B., Morsi, B.I., Heier, K.R., Machado, R.M., 2002. Industrial and Engineering Chemistry Research 41, 697–709.

Flowers, R.A., Naganathan, S., Dowd, P., Amett, E.M., Ham, S.W., 1993. Journal of the American Chemical Society 115, 9409–9416.

Furusjö, E., Danielsson, L.G., 2000. Chemometrics and Intelligent Laboratory Systems 50, 63–73.

Furusjö, E., Svensson, O., Danielsson, L.G., 2003. Chemometrics and Intelligent Laboratory Systems 66, 1–14.

Hairfield, E.M., Moonmaw, E.W., Tamburri, R.A., Vigil, R.A., 1985. Journal of Chemical Education 62, 175–177.

House, H.O., 1972. Modern Synthetic Reactions, 2nd ed. Menlo Park, California, W.A. Benjamin, Inc., pp. 306–310.

HyperChem, 2002. Version 7.0, CompuChem: http://www.compuchem.com.

Karlsen, L.G., Villadsen, J., 1987. Chemical Engineering Science 42, 1153–1164.

Landau, R.N., 1996. Thermochimica Acta 289, 101–126.

Landau, R.N., McKenzie, R.F., Forman, A.L., Dauer, R.R., Futran, M., Epstein, A.D., 1995. Process Control and Quality 7, 133–142.

LeBlond, C., Wang, J., Larsen, R., Orella, C., Sun, Y.K., 1998. Topics in Catalysis 5, 149–158.

Levenspiel, O., 1998. Chemical Reaction Engineering, 3rd ed. Wiley, New York.

Ma, B., Gemperline, P.J., Cash, E., Bosserman, M., Comas, E., 2003. Journal of Chemometrics 17, 470–479.

Machado, R.M., Mitchell, J.W., Bullock, J.P., Farrell, B.E., 1996. Thermochimica Acta 289, 177–187.

Maeder, M., Zuberbühler, A.D., 1990. Analytical Chemistry 62, 2220–2224.

Matlab Optimization Toolbox, Version 2.1 (R12), Mathworks: www.mathworks.com/products/optimization

Mayes, D.M., Kelly, J.J., Callis, J.B., 1992. In: Hildrum, K.I., Isaksson, T., Naes, T., Tandberg, A. (Eds.), Near Infra-Red Spectroscopy Bridging the Gap between Data Analysis and NIR Applications. pp. 377–387.

Moore, H.W., 1967. Journal of Organic Chemistry 32, 1996–1999.

NIST, 2003. NIST Chemistry Webbook. Standard Reference Database Number 69, online, National Institute of Standards and Technology.

Nomen, R., Sempere, J., Avilés, K., 2001. Chemical Engineering Science 56, 6577–6588.

Regenass, W., 1997. Chimia 51, 189–200.

Ubrich, O., Srinivasan, B., Lerena, P., Bonvin, D., Stoessel, F., 1999. Journal of Loss Prevention in the Process Industries 12, 485–493.

Zogg, A., 2003. A combined approach using calorimetry and IR-ATR spectroscopy for the determination of kinetic and thermodynamic reaction parameters. Diss. ETH No. 15086, ETH Zürich, http://e-collection.ethbib.ethz.ch/cgi-bin/show.pl?type = diss&nr = 15086.

Zogg, A., Fischer, U., Hungerbühler, K., 2003. Industrial and Engineering Chemistry Research 42, 767–776.

Zogg, A., Fischer, U., Hungerbühler, K., 2004a. Chemometrics and Intelligent Laboratory Systems 71, 165–176.

Zogg, A., Stoessel, F., Fischer, U., Hungerbühler, K., 2004b. Thermochimica Acta 419, 1–17, (doi:10.1016/j.tca.2004.01.015).